



UNIVERSITÀ DEGLI STUDI DI PADOVA

Department of General Psychology

Bachelor's Degree Course in Psychological Science

Final Dissertation

**The Role Of Frontal Eye Fields In
The Inhibitory Tagging Mechanism:
A Study With Transcranial Magnetic Stimulation**

Supervisor:
Professor Gianluca Campana

Candidate:
Simone Ghini

Student ID Number:
2033411

Academic Year 2023/2024

Table of Contents

| | |
|---|----|
| Abstract..... | 5 |
| Abstract in Italian..... | 6 |
| 1. Introduction..... | 8 |
| 1.1 Attention | 8 |
| 1.2 Visual Attention..... | 9 |
| 1.2.1 Neural correlates: Frontal Eye Fields | 12 |
| 1.2.2 Inhibitory Tagging Mechanism..... | 15 |
| 2. The Multi-Item Localization Task..... | 20 |
| 3. Transcranial Magnetic Stimulation..... | 23 |
| 4. Purpose of the Study | 27 |
| 5. Methods..... | 28 |
| 5.1 Participants..... | 28 |
| 5.2 Equipment and Stimuli | 29 |
| 5.2.1 MILO 2022 Version..... | 29 |
| 5.2.2 Magstim Rapid ² TMS and Neuronavigation..... | 31 |
| 6. Experimental Procedure and Design..... | 34 |
| 7. Results..... | 37 |
| 7.1 Factor 1 - Target Number | 38 |
| 7.2 Factor 2 - Vanish-Remain condition..... | 42 |
| 7.3 Factor 3 - Time..... | 42 |
| 7.4 Analysis of interaction effects | 43 |
| 7.5 Analysis of the slopes | 44 |
| 8. Discussion and Conclusions | 46 |
| 9. References..... | 48 |

Abstract

The Inhibitory Tagging Mechanism has been proposed as the system responsible for impeding the reorientation of attention to previously visited locations or items. Accumulating evidence suggests that its neural underpinnings are located in the Frontal Eye Field (FEF) neurons in mammals.

In the present study, we aimed to investigate the nature of this phenomenon which was elicited using the Multi-Item Localization (MILO) Task. The MILO task is a visual search task whereby participants are asked to select, according to a given order, a number of targets in sequence. Selection can occur via tapping on a screen or clicking with a mouse, and the order is typically given by increasing numbers (e.g., from 1 to 8) attached to each target item.

There are two conditions: in one condition each item disappears upon selection (*Vanish*), in the other condition no item disappears upon selection (*Remain*). Serial reaction times (SRTs), that is the times needed to select each successive item in the sequence, are measured.

Previous studies have demonstrated that SRTs decrease with increasing selected target items in the sequence for both the *Vanish* and *Remain* conditions. For the *Vanish* condition this can be explained by a decrease in set size with increasing target number, whereas for the *Remain* condition this indicates the presence of inhibitory tagging.

By reducing the cortical excitability of FEF using offline 1 Hz Transcranial Magnetic Stimulation (TMS), we expect to observe a divergent pattern between the curves describing SRT as a function of target number (i.e., $SRT \times \text{target number}$ function) for the *Vanish* and *Remain* conditions.

Our analysis produced results consistent with the literature, confirming the characteristic pattern of the curves prior to stimulation. However, there is no evidence indicating that TMS had a causal effect in suppressing the inhibitory tagging mechanism. Consequently, this study does not allow us to conclude that this mechanism is localized within the FEF areas.

Abstract in Italian

Il sistema di “tagging inibitorio” è stato proposto come il sistema responsabile per impedire il riorientamento dell’attenzione verso posizioni spaziali o oggetti precedentemente osservati. La letteratura esistente attribuisce questo meccanismo a popolazioni di neuroni situati nei campi oculari frontali (frontal eye fields - FEF).

Per analizzare il suddetto meccanismo, è stato usato un compito di ricerca visiva, il Multi-Item Localization (MILO) Task. Il compito consiste nel selezionare, secondo un ordine prestabilito, una serie di target, in sequenza. La selezione può essere effettuata toccando i target su uno schermo touch-screen o cliccando con il mouse. Un numero viene assegnato a ciascun target e l’ordine prestabilito è solitamente di tipo numerico e crescente (ad esempio, da 1 a 8).

Il MILO contiene due condizioni: in una, ogni target scompare quando viene selezionato (*Vanish*); nell’altra, tutti i target rimangono sullo schermo anche dopo essere stati cliccati (*Remain*).

Per ogni trial vengono misurati i cosiddetti tempi di reazione seriale (serial reaction times – SRTs), ovvero il tempo necessario per selezionare ogni target successivo.

Diversi studi hanno riportato che i SRTs diminuiscono con l’aumentare del numero di target selezionati nella sequenza, in entrambe le condizioni. Per la condizione *Vanish*, questo accade in quanto il numero di oggetti presenti sullo schermo diminuisce con l’aumentare del numero di target, mentre per la condizione *Remain* è indicativo dell’attivazione del sistema di “tagging inibitorio”.

Andando a inibire l’attività dei neuroni dei campi oculari frontali tramite stimolazione magnetica transcranica (Transcranial Magnetic Stimulation – TMS) a 1 Hz in modalità offline, ci aspettiamo

di osservare una divergenza tra le curve che descrivono l'andamento dei SRT in funzione del numero di target, nelle due condizioni.

In fase di analisi, è stato possibile riscontrare risultati in linea con la letteratura, confermando il caratteristico andamento delle curve prima della stimolazione. Tuttavia, non vi è sufficiente evidenza per indicare che la TMS abbia avuto un ruolo causale nella soppressione del sistema di "inhibitory tagging". Di conseguenza, con i risultati di questo studio non è possibile concludere che tale meccanismo sia effettivamente localizzato nelle aree dei campi oculari frontali.

Keywords: Frontal Eye Fields (FEF), Inhibitory Tagging Mechanism, Multi-Item Localization (MILO) Task, Transcranial Magnetic Stimulation (TMS)

1. Introduction

1.1 Attention

Attention is a cognitive function that involves selecting and identifying certain stimuli in the environment while disregarding others.

The need for selectivity responds to two fundamental limitations: physiological and processing constraints.

The former refers to the high metabolic demand that the brain has on the body. The physical constraints of blood supply to the brain pose a limit to the amount of electrical signaling that can be generated by cortical neurons and in turn, to the amount of sensory information that can be processed simultaneously. Thus, the brain's limited energy resources must be allocated flexibly to neuronal cells according to specific task demands over time. In this view, the switching of energy resources between different regions translates into the switching between cognitive tasks, which is manifested as attention (Mather, 2016).

The latter indicates a limitation that is intrinsic to the information-processing theory of the mind adopted by cognitive theories. Accordingly, the brain has a maximum communication capacity that cannot be exceeded and attention behaves as a filter, reducing and selecting the most salient features of the sensory world that would otherwise overwhelm the system. This conceptualization of attention was proposed by Donald Broadbent, who in 1958 postulated the filter model of attention. Several theories have followed based on different implementations of the filter, but the process at the basis, driven by the brain's limited processing capacity remains a core feature in the modern theories, too.

1.2 Visual Attention

Visual attention is the mechanism the nervous system uses to highlight specific locations, objects or features within the visual field (Bisley, 2010). Most research has focused on the orienting of visual attention and the influence that top-down and bottom-up factors have on it. In fact, these two main types of factors are crucial in influencing visual attention and, more broadly, perceptual experiences.

On one hand, top-down processing utilizes contextual information, prior knowledge, expectations, and goals to interpret sensory information coming from the external sensory world. On the other hand, bottom-up processing is solely driven by external sensory stimulation, and it is the dynamic interplay between them that guides and orients visual attention.

Evidence from behavioral, neuroimaging, electrophysiological, and lesion studies indicates that two partially segregated neural systems subtend the processing of these factors in the allocation of visual attention. The review published by Corbetta and Shulman in 2002 collected and analyzed these findings, initially suggesting the existence of dorsal and ventral attentional networks in the frontoparietal regions of the brain. Collectively, these are referred to as the frontoparietal attentional network.

The dorsal attentional network (DAN) is responsible for the top-down, goal-directed control of visual attention. From fMRI studies it is evident that there is a sustained activation of the intraparietal sulcus (IPS) and the frontal eye fields (FEF) whenever attention to a specific spatial location is cued (i.e., the top-down factor). For instance, in one study by Corbetta et al. (2000) subjects were presented an arrow cueing one of two possible locations (left or right) and instructed to covertly (without moving their eyes) shift their attention to the indicated location in preparation for the target. Results have shown transient activation in the occipital areas, most likely due to

general processing of visual information, and more importantly sustained activation of the DAN that was time-locked to the period in which they had to pay attention to the cue.

As for overt orienting of attention, saccadic eye movements are required to shift the gaze to a particular spatial location and the time-locked activity of neurons prior to the oculomotor response is thought to represent the engagement of an attentional mechanism. In several studies that used visual search paradigms, researchers were able to relate neural activity in the DAN, both in the IPS and in the FEF, to the generation of a saccade showing its contribution in overt attentional shifting, too. Finally, a more recent review by Vossel et al. (2013) confirmed that the DAN is a bilaterally organized network that becomes active in both covert and overt allocation of attention, mediating top-down processing.

Conversely, the ventral attentional network (VAN) is recruited in processing bottom-up factors that influence the orientation of attention and has its neural correlates in the temporoparietal junction (TPJ) and the ventral frontal cortex (VFC) of the right hemisphere. In real life, these bottom-up factors function as distractors that interrupt ongoing cognitive processing of the environment. For example, a fast-moving emergency vehicle with flashing lights suddenly appearing in the periphery of our visual field can abruptly redirect our attention, even if we were focused on crossing the street. In laboratory settings, analogous bottom-up (stimulus-driven) factors can be simulated by presenting targets at unexpected locations.

Although the DAN is most engaged in redirecting covert and overt attention to a specific spatial location, the VAN does not operate in the same manner. In fact, according to Corbetta and Shulman (2002) its activation is more generally modulated by the detection of unattended or low-frequency events, independent of their location, sensory modality of presentation or response demands.

It is also worth noting that the role of the TPJ is still unclear since it participates in many other cognitive functions and may not be solely responsible for attentional reorienting. In addition, it is not only involved in bottom-up processing since it was observed that this area is engaged in contextual cueing paradigms when salient nontargets in a visual search provide information about a target. This may suggest that this area of the VAN is not simply stimulus-driven, but participates in an early integration of relevant contextual information which may be later transmitted to the dorsal regions to implement an attentional reorienting.

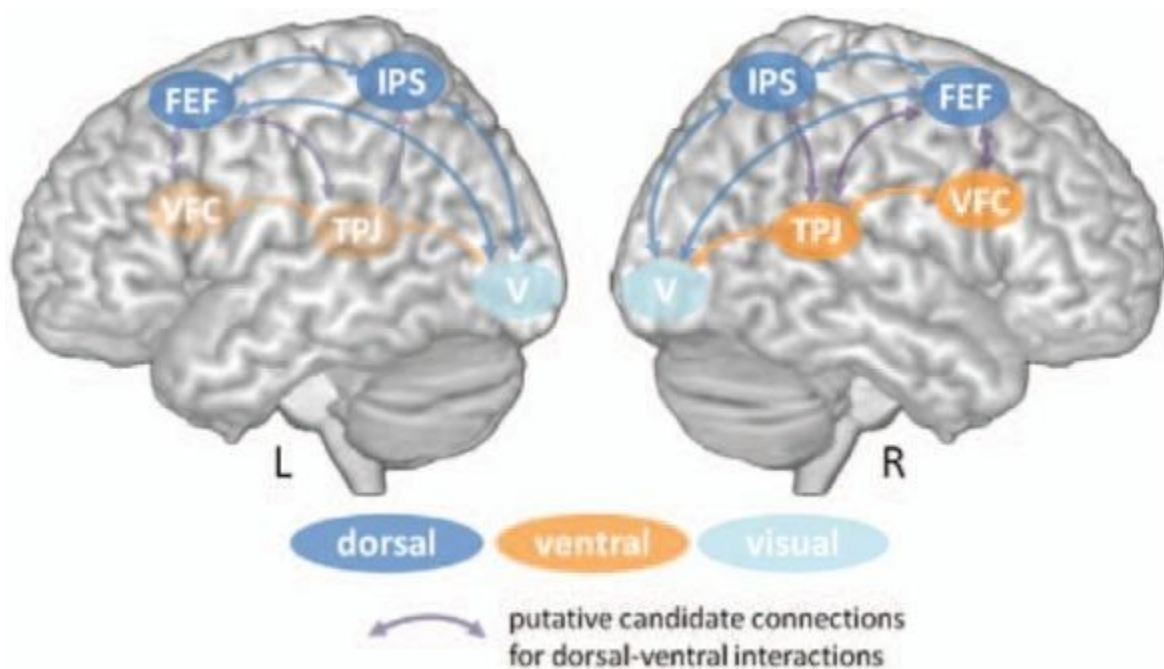


Figure 1. Taken from Vossel et al. (2013). The diagram shows the components of the dorsal (blue) and ventral (orange) attention systems in the human brain. The left VAN is slightly faded to reflect the stronger evidence supporting its right lateralization. The arrows indicate potential intra- and inter-network connections. Abbreviations: FEF = frontal eye fields; IPS = intraparietal sulcus; VFC = ventral frontal cortex; TPJ = temporoparietal junction; V = visual cortex.

1.2.1 Neural correlates: Frontal Eye Fields

The frontal eye fields (FEF) are considered to be a crucial hub region within the dorsal attentional network, attracting significant interest due to their functional contribution to visual attention in both healthy and diseased states, such as visuo-spatial neglect. Indeed, nearly half of right-hemisphere stroke survivors suffer from this debilitating neuropsychological disorder, which involves a lack of visual awareness and impaired attentional orienting to the contralateral visual field (Barrett, 2021). Indeed, neglect is essentially an attentional disorder, making it of crucial importance to investigate not only the attentional networks as a whole, but also their constitutive components with a detailed and nuanced approach (Corbetta & Shulman, 2002).

A pivotal element in this search revolves around the precise location of the frontal eye fields. The localization of the FEF has been the subject of extensive research over the years, beginning with microlesion studies with animal models and progressing to human research involving neuroimaging and non-invasive brain stimulation techniques with the aim of finding a corresponding area.

In non-human primates, the FEF are functionally defined as the portion of the dorsolateral prefrontal cortex from which low intensity intracortical stimulation elicits rapid eye movements (Vernet et al., 2014).

In humans, neuroimaging studies using PET, fMRI, and MEG report similar results in locating the FEF along the precentral sulcus in the frontal lobe, near the junction with the superior frontal sulcus within Brodmann's Area 6, with some variability along the rostral-caudal axis between humans and monkeys (Vernet et al., 2014).

Despite the great advances that have been made over the years, there is still some inconsistency in the results due to inter-individual variability and the different methodologies and paradigms used to identify their location.

As for the role of the FEF, they are mainly implicated in the programming and triggering of voluntary eye movements, such as voluntary saccades. In fact, lesion studies have provided evidence for their specific contribution to the voluntary component of oculomotor movements, leaving the control of involuntary (reflexive) saccades to areas in the posterior parietal cortex, namely the parietal eye fields (PEF). Nonetheless, the existence of several pathways connecting the FEF, the PEF, and other areas involved in eye movements, such as the superior colliculi (SC), led to the hypothesis of context-dependent modulatory effects on reflexive saccades, too.

Furthermore, other studies showed their involvement in the control of other types of ocular movements, such as smooth pursuit, optokinetic nystagmus, vergence, but also fixation (Vernet et al., 2014). Tiny subregions within the FEF are activated depending on which ocular behavior is being engaged, which makes it even more difficult to identify their precise location in humans.

The function of the FEF extends beyond ocular movements per se to include more cognitive aspects of vision, such as participating in the orienting of both covert and overt attention. Notably, a study by Wardak et al. (2006) investigated this dual role using two different behavioral tasks with a microinjection of muscimol (GABA_A agonist) in the FEF area of monkeys to reversibly deactivate it.

In the task testing overt attention, monkeys performed a visually guided saccade task where they had to make a saccade towards a target among eight items and maintain fixation on it for 1000ms. Results showed that the latency of the contraversive and ipsiversive saccades increased significantly from the control to the injection condition in both monkeys.

In the covert attention task, monkeys were required to maintain their gaze on a fixation point for the whole duration of the trial and up to three visual search displays appeared in succession, and if a target was present, they had to press a lever within 900 ms after its presentation. The data indicated that FEF inactivation produced longer reaction times for contralesional targets, but not for the ipsilesional ones. The findings present evidence that the FEF are not simply involved in ocular movements but in attentional orienting, too.

The investigation of their function in humans began with the study of clinical patients with lesions following a diverse range of brain pathologies which has provided initial insights into the contributions of the area to vision, yet it is unlikely that these lesions were solely confined to the FEF, making it difficult to isolate their specific involvement. For this reason, non-invasive techniques like TMS, which modify the excitability of neurons in cortical areas with high spatial resolution, have become the gold standard for analyzing the function of the human FEF. Thanks to these advances, it was possible, for instance, to provide direct causal evidence of the presence of a saliency map for the selection of an upcoming target within the area of the human FEF (Walker et. al 2009).

A priority map is a cognitive representation of the visual environment that operates by assigning varying levels of priority to items, objects, or locations based on their attentional significance (Bisley, 2010). Within these maps, certain areas are inhibited while others are positively enhanced; the computation of all the “weights” in these maps determines the spatial location with the highest priority, directing covert or overt attention to it.

In Walker and colleagues’ study they showed how stimulation of the right FEF disrupted the enhancement of target salience on an endogenous saccade task, proving once again the involvement of the FEF in attentional mechanisms.

Of particular relevance to this discussion is their involvement in the inhibitory tagging mechanism, which will be further examined in the next section.

1.2.2 Inhibitory Tagging Mechanism

Inhibition of Return (IOR) is an attentional effect whereby response times to a previously cued location are longer compared to those to an uncued location. This phenomenon was discovered in 1984 by Posner and Cohen, who first observed it with the classic cue-target paradigm, later referred to as the Posner cueing task (Fig. 2a). The prototypical trial includes a fixation frame with three boxes aligned on a horizontal line equally spaced apart, one at center and the others at the periphery. A cue (S1) may be presented at one of the two peripheral locations, and then the fixation frame is shown again. After a varying time interval, a target (S2) appears at either the cued or uncued location and participants are required to give a response about the position of the target. The time interval is called the cue-target onset asynchrony (CTOAs) and has different durations, typically ranging from 0 ms up to 500 ms. Posner and Cohen observed a facilitatory effect for cued targets with CTOAs below 200-250 ms, however beyond this crossover point, response times gradually increased and facilitation transitioned to inhibition. This phenomenon, characterized by longer reaction times for cued targets in the trials with CTOAs exceeding 200-250 ms, was termed inhibition of return. Noteworthy is the fact that trials with CTOAs higher than this threshold showed longer response times for previously cued targets even when compared to uncued targets, contrary to the earlier observed facilitatory pattern (Fig. 2b).

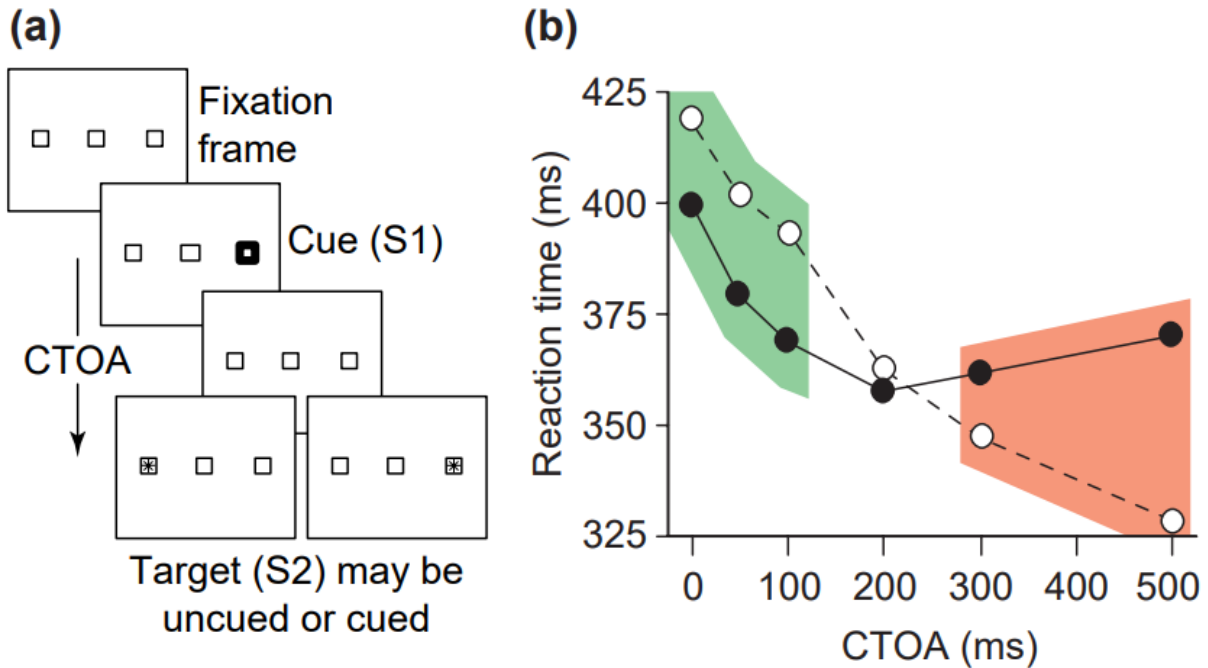


Figure 2a depicts the sequence of frames in the Posner cueing task.

Figure 2b reports the graphs for cued targets (filled dots) and uncued targets (blank dots). The facilitatory effect observed below the crossover point is within the green area, while the inhibitory effect (IOR) is shown in the red area. With CTOAs ≥ 250 -300 ms the pattern is reversed, with response times for uncued targets becoming shorter than those for cued targets.

Both figures are taken from Klein (2000).

The analysis was taken to a further extent in an attempt to explain the functional significance of the existence of such a mechanism. Klein (1988) expanded the study of IOR from the Posner cueing tasks to visual search tasks and showed that it operated as a facilitator of visual foraging behavior. Within this theoretical framework, the IOR is conceptualized as a mechanism that tags locations or items already searched and designated as non-targets. This tagging assists in directing attention to the next stimulus to be scanned, ensuring that only new, previously unsearched

locations in the array are examined. It is by preventing the re-examination of areas that have already been marked as non-targets, that the inhibitory tagging mechanism expedites the visual search process.

It is also worth noting that this facilitation does not apply to easy/parallel search tasks, as these do not involve attentional orienting mechanisms. Instead, they rely on a simultaneous analysis of the entire array of stimuli.

The implementation of the inhibitory tagging mechanism in the brain seems to lie within the FEF area. As previously mentioned, the FEF is engaged in saccadic programming, priority maps, and attentional reorienting which are all required during a search task. The study of the neural correlates of the mechanism in primates was carried out by Mirpour et al. (2019) where they recorded the activity of 231 neurons in the FEF of two rhesus macaques during a visual foraging task. They hypothesized that within this group of neurons there would be a subset that specifically coded for the inhibitory tagging mechanism and named them putative tracking neurons. These neurons were selected according to two criteria:

- they should have preferentially responded to previously fixated items;
- their activity should have not been suppressed during maintained fixation.

The second criterion was essential because, most neurons in the FEF area show activity levels close to the baseline during fixation, possibly representing a flattening of the priority map. Instead, the putative tracking neurons are required to do the exact opposite, they should somehow change the “weights” of the spatial locations in the priority map and guide saccades away from previously searched areas.

The experimental paradigm used to test their hypothesis consisted of a visual foraging task whereby animals fixated on a starting point, after which an array of ten stimuli — five potential

targets and five distractors — appeared. Only one of the five potential targets was linked to a juice reward, obtained by fixating on it for at least 500 ms. The position of the targets and the distractors was randomly assigned in each trial. Findings revealed two main patterns of fixation duration when a potential target was within the fovea.

The first pattern, involving fixations shorter than 500 ms, occurred similarly regardless of whether the stimulus had been previously fixated or not. However, in this quick fixation pattern, there was a significantly greater amount of fixations to previously viewed stimuli than to those not yet fixated. This suggests that when a stimulus had been fixated before, in most cases, the two monkeys tended to use this fast fixation approach to quickly shift their gaze away from one stimulus to the next.

In the second, slower pattern, which occurred when animals fixated on stimuli for longer than 500 ms, the duration was significantly shorter for previously fixated stimuli compared to non-fixated ones.

In both cases, there seems to be evidence of the presence of a mechanism that keeps track of the previously searched stimuli and that could correspond to the aforementioned inhibitory tagging.

The neuronal recordings also helped corroborate their predictions: putative tracking neurons were indeed activated during maintained fixation, unlike the rest of the FEF neuronal population analyzed.

Based on the evidence supporting the presence of the inhibitory tagging mechanism in the primates' FEF area, in our study we hypothesized that a similar mechanism would be found in the corresponding brain region in humans.

In order to investigate this phenomenon, we used a different visual search paradigm, namely the Multi-Item Localization (MILO) Task and to infer causality we employed the non-invasive brain stimulation method known as Transcranial Magnetic Stimulation.

The next two sections will provide an overview of both the MILO Task and TMS, highlighting their relevance to our experiment.

2. The Multi-Item Localization Task

The Multi-Item Localization (MILO) Task is a visual search task conceived to bridge the gap between the traditional tasks used in laboratory settings and real-life visual search. It was first presented in a paper by Thornton and Horowitz (2004), where they proposed this novel method to uncover the spatiotemporal context in search tasks.

In the first experiments using the MILO, each trial began with a *cue* phase where four target letters in alphabetic sequence were presented. The participants could look at the sequence for as long as they wanted, before starting the *search* phase. In this part, the display contained both the targets and four additional distractor letters. The participants were instructed to locate and subsequently click on the target letters in sequence.

The ability to make direct responses by clicking with a mouse, differentiates the MILO from most other visual search tasks, where participants usually have to respond indirectly by reporting whether or not a target is shown. Indeed, in real life, we categorize, navigate, pick up, and generally interact with objects we view, which is what this tool attempts to recreate, thereby improving the external validity of the experimental design.

The key measure in the task, serving as the dependent variable, is the Serial Reaction Time (SRT), which measures the time taken by the individual to locate each successive target. More precisely, the SRT is defined as the time interval elapsed between the click on target n and the click on the following target, $n - 1$.

The MILO allows the examination of both retrospective and the prospective component of the visual search. Understanding the retrospective component means utilizing the tool to comprehend whether or not the localization of the current target affects the search for the subsequent one. In

other words, they were essentially examining if "where you've been" impacts "where you're going."

The two different conditions *Vanish* and *Remain* had exactly this purpose. As briefly mentioned in the abstract, in the *Vanish* condition, each target disappears once it is clicked upon, whereas in the *Remain* condition, it stays visible even when selected. Since the set size in the *Vanish* condition progressively decreases, we would expect faster reaction times compared to the other condition, where clicked items become distractors as the number of items diminishes.

Instead, data shows similar SRTs acceleration patterns in the two conditions as evidenced by Fig. 3 below.

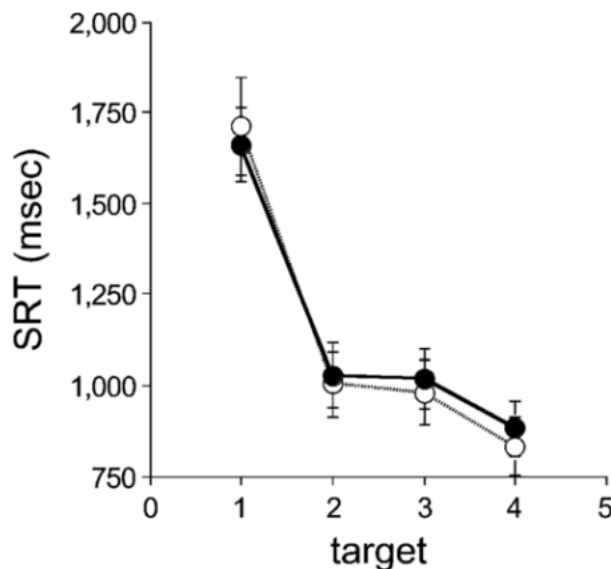


Figure 3. Taken from Thornton and Horowitz (2004). SRT \times target number function. The Remain condition is indicated by filled dots and the Vanish condition is represented with blank dots. The error bars indicate standard errors of the means.

From the graph and the analysis conducted by Thornton and Horowitz (2004) it is possible to infer that there is some type of inhibition of previously searched locations that occurs in the *Remain* condition that could explain the similar curve patterns. Physically removing the targets after being clicked or not doing so, did not have an influence on the SRT as a function of the target number in the sequence. Furthermore, the slightly accelerating profile of the SRT \times target number function

indicates that inhibition persists as the task progresses, with previously searched locations not regaining spatial priority. The findings are consistent with Klein's theoretical formulation of the inhibitory tagging mechanism, thus justifying the use of the MILO in our experiment to further investigate this phenomenon.

3. Transcranial Magnetic Stimulation

Transcranial Magnetic Stimulation (TMS) is a non-invasive method to generate an electrical current in the brain, thereby modifying cortical excitability, making it valuable in both research and clinical settings (Rossini et al., 2015).

The key principle in the functioning of TMS is Faraday's Law of electromagnetic induction (1831), which states that a rapidly changing magnetic field (B-field) induces an electric current (E-field) in a nearby conductor, typically oriented perpendicular to the magnetic field.

The implementation of the law in the TMS equipment is obtained by passing a brief electric current into a copper wire coil which in turn generates a magnetic field (B-field) of about 1-2 T, comparable to the field produced by an MRI machine.

By applying the coil to the scalp, the magnetic field can pass through the skull bone and induce local hyperpolarization or depolarization of the cortical neurons' membranes through the generated electric field (E-field). Therefore, the stimulation itself is ultimately electrical in nature, but it is mediated by a magnetic field (Koponen & Peterchev, 2020).

The application of electrical current directly to the scalp is possible, with Transcranial Electrical Stimulation (TES) devices, however TMS has proven to be a more suitable and safer method for various applications especially those requiring a better spatial resolution.

Unlike TES, TMS coils can have different shapes, each determining a different area of stimulation.

The most basic type is a round circular coil that induces a circular electrical field on the stimulated area. However, the need for a focal and precise stimulation of specific brain areas, led to the development of the figure-of-eight structure which became the most commonly used type of coil.

In this configuration two circular windings are positioned next to each other with the current

flowing in each of them in opposite directions, thereby inducing the most intense electric stimulation at the point where the two circles meet (Lefaucheur, 2019).

The coil type is not the only factor that influences the effects of TMS on neurons, another crucial factor is the current pulse waveform that flows through the coil which determines the type of neural circuitry that is stimulated by the coil.

There are two main categories of pulse waveforms: monophasic and biphasic.

In a monophasic pulse, an intense initial current is required and it is subsequently reduced by a dampened return current. Stimulation in the brain occurs only during the initial part of the pulse; the reverse current does not affect this stimulation.

In a biphasic pulse, there is a double reversion of the current, with both phases being able to induce physiological changes at neuronal level. These pulses produce a more intricate pattern of neural activation and stimulate a more diverse group of neurons compared to monophasic pulses. Additionally, because they require less energy to function, they are primarily used in repeated transcranial stimulation protocols (rTMS).

Indeed, there are various TMS protocols, including single pulse, paired pulse, and pulse trains.

In single pulse TMS, a single pulse is discharged at a time, usually to assess Motor Evoked Potentials (MEPs) using electromyographic (EMG) recordings. MEPs are electrical responses from muscles following motor cortex stimulation, evaluating the integrity of the corticospinal tract and motor pathways. This method provides essential insights into motor cortex function and is fundamental for diagnosing neurological disorders and guiding interventions.

In paired-pulse TMS, two pulses are delivered with an interval ranging from 1 ms to 250 ms and it allows for the study of the connectivity between two different brain regions when two coils are used, or for the analysis of the neural circuits involved with intracortical inhibition and facilitation.

Pulse trains are those associated with rTMS, which consists in the delivery of a series of pulses (trains) in a repetitive manner at a specified frequency. The use of this protocol requires a quick recharge of the stimulator, which can easily be obtained by using a biphasic pulse.

rTMS has a long-lasting neuromodulating effect that continues after the period of the stimulation that can either be inhibitory or excitatory (Fig. 4).

Low frequency rTMS at ≤ 1 Hz, consists of continuous trains of single pulses that are thought to inhibit the cortical areas stimulated, however results are mixed and highly contradictory (Rossini et al., 2015).

On the other hand, high frequency rTMS (5-20 Hz) studies report observing facilitatory effects, with robust evidence for stimulation of the motor cortex.

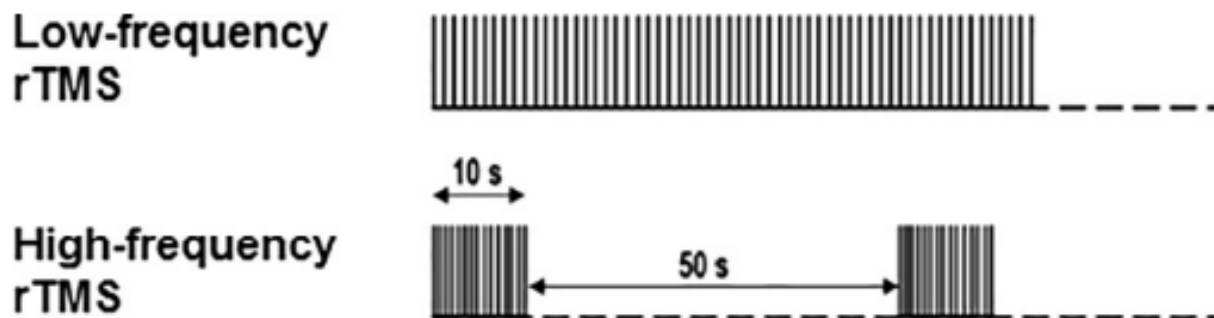


Figure 4. Adapted from Lefaucheur (2019). The top section illustrates the low frequency rTMS paradigm (≤ 1 Hz), while the bottom section shows the high frequency rTMS paradigm (5–20 Hz).

Proper localization of the brain area to be stimulated is essential for the effective use of TMS and this is made possible by neuronavigation.

A common approach to neuronavigation is to follow a functional localization method: mapping specific brain regions responsible for certain functions by applying targeted stimulation and observing the corresponding physiological or behavioral responses. For example, we should expect the production of movements following the stimulation of the precentral gyrus, or the presence of phosphenes when the occipital cortex is stimulated (Lefaucheur, 2019).

When multiple stimulation sessions are scheduled over several days, and repetitive targeting of the same brain area is required, it is recommended to use more precise and sophisticated neuronavigation methods. For instance, in our experiment, we utilized a frameless optic neuronavigation system, which included an infrared Polaris camera and multiple trackers to precisely identify the areas targeted for stimulation. This was facilitated by the Brainsight TMS Navigation system, a computer software that enabled three-dimensional visual navigation for accurate localization of the FEF area using the Montreal Neurological Institute (MNI) coordinate system.

4. Purpose of the Study

As previously mentioned, the FEF area is within an attentional network dedicated to the top-down processing of stimuli orienting visual attention. The study of the neural correlates of the inhibitory tagging mechanism conducted on mammals by Mirpour et al. (2019) suggested the existence of putative tracking neurons carrying this exact function in rhesus monkeys. In this study, we postulated the neural underpinnings of this mechanism to be in the human's FEF. Previous findings from the MILO task, showed that inhibitory tagging is activated in the *Remain* condition and we propose to interfere with it by using rTMS at 1 Hz in order to obtain an inhibitory effect. By inhibiting the FEF area we hypothesized to observe the SRT \times target number function of the two conditions to have different accelerations (slopes) as the task progresses (i.e., the number of targets decreases). Particularly, by reducing the effect of the inhibition of previously searched locations, we expect to observe a slower acceleration profile in the *Remain* condition than in the *Vanish* condition.

The experimental design is a repeated-measure design whereby every participant was tested on each condition, providing their own control.

5. Methods

5.1 Participants

For the study, a total of 12 (7 females and 5 males) participants with an age range between 19 and 25 was recruited among Psychology students at the University of Padova. The experiment was approved by the Local Ethics Committee (Comitato Etico di Psicologia dell'Università di Padova) following a thorough evaluation adhering to international ethical guidelines for research involving human subjects.

An informed consent compliant with these standards was redacted and provided to all participants before the study began.

The document provided information on the handling of personal and experimental data, the experimental design, the possibility to withdraw from the study at any time, and the guarantee of anonymity.

In a specific section of the informed consent form, a brief explanation of the mechanism underlying the use of TMS and rTMS was included along with its potential risks.

All participants declared to have normal or corrected to normal vision and additional medical exclusion criteria were verified through a questionnaire attached to the informed consent.

The TMS safety questionnaire was created according to the content outlined in “Safety and recommendations for TMS use in healthy subjects and patient populations, with updates on training, ethical and regulatory issues guideline” by Rossi et al. (2021).

Participants were required to have no history of psychiatric or neurological conditions, epilepsy, fainting or syncope, traumatic brain injury (TBI) with loss of consciousness, hearing issues including tinnitus, or cerebrovascular problems. They also had to declare that they were not pregnant, did not have metal implants in the brain or other body parts, and were not carrying brain

or spinal stimulators, or pacemakers. Only those who had not recently received transcranial magnetic stimulation or undergone magnetic resonance imaging were included in the study. Additionally, they were instructed to refrain from consuming more than two coffees (or equivalent caffeine intake), more than two units of alcohol, and any narcotics in the 24 hours prior to each experimental session.

The completion of all three experimental sessions granted a compensation of 25€ funded by the University.

5.2 Equipment and Stimuli

5.2.1 MILO 2022 Version

The behavioral data collection was performed using the MILO Task. The version of the MILO Task used in the experiment was an updated form of the one presented in the seminal papers by Thornton and Horowitz. In this newer version, the task was presented on a web app, but the goal remained the same: to click through the sequence of targets as quickly as possible in the correct order.

Unlike the original version, which used letters, the display consisted of eight pool balls, each labeled with a number from 1 to 8. Participants were required to click on these balls in ascending order using a mouse. See Fig. 5 for reference.

The task started with a practice block composed of four trials to help them become familiar with the *Vanish* and *Remain* conditions. Immediately after, the main block of 32 trials began, consisting of an equal mix of 16 *Vanish* and 16 *Remain* trials that were randomly intermixed in the experimental block.

Whenever an error was made, the trial ended and it was moved to the end of the block ensuring that the experimental block of each participant had a total of 32 trials.

A visual feedback was provided at the end of each trial: for correct trials, the trial completion time was displayed, while for incorrect trials, a message appeared stating "Oops! That was incorrect!" The feedback display did not have a fixed duration and participants could decide whenever they wanted to proceed by clicking the "Continue" button at the center of the screen.

The task was shown on a 24'' computer screen with a resolution of 1920x1080 pixels.

Each ball had a diameter of 85 pixels and participants were positioned on a chin rest at 68.5 cm from the screen. With this setup, each ball subtended approximately 1.8° visual angle.

In this version, neither the *cue* phase nor the fixed distractors were included. However, every ball except for the subsequent one is assumed to act as a distractor, thereby triggering the inhibitory tagging during the visual search. For example, while searching for ball #2, all other balls are considered distractors, except for ball #3.

The software automatically collected the reaction times of each trial which were later available to be stored for further analysis.

The total duration for the behavioral data collection was approximately 10-15 minutes, followed by TMS stimulation. Later, it was repeated with another round of behavioral data collection to assess pre- and post- stimulation differences for each participant and session.



Figure 5. Example of a MILO Task trial as it appeared to participants during the experiment.

5.2.2 Magstim Rapid² TMS and Neuronavigation

The TMS model adopted in the current study was a Magstim Rapid² with an air-cooled, figure-of-eight coil that was used to stimulate three different areas: left FEF (lFEF), vertex (Cz), and right FEF (rFEF).

Stimulation of both left and right FEF was performed to explore functional lateralization of the areas and it was carried out using neuronavigation methods.

The control site (i.e., Cz) was found using the International 10-20 System.

The localization of the FEF areas was determined during each session through a frameless optic neuronavigation procedure, which uses a position sensor camera (Polaris) to precisely localize the position of three trackers, each equipped with three spheres that reflect the infrared light emitted by the camera (Fig. 6a). These reflections are then detected along the x , y , and z axes, enabling real-time localization in the 3D space.

The subject tracker (Fig. 6b) was secured onto the participant with a head-strap, the coil tracker was attached to the TMS coil, and lastly, the neuronavigation tracker (Fig. 6c) was used to identify key anatomical landmarks required for the modeling of the participant's skull on the computer software Brainsight. The version we utilized (2.3.8) supports the use of the person's own MRI scans or, as it was in this case, the template brain provided by the Montreal Neurological Institute (MNI).

The MNI 152 coordinates system is a standardized template obtained by averaging the MRI scans of 152 healthy brains, serving as a common framework to map brain structures independently of inter-individual morphological variability.

In the current study, the MNI coordinates of the left and right FEF were based on a meta-analysis published by Bedini et al. (2023), which located them at:

- Left FEF: ($x = -26, y = -6, z = 54$)
- Right FEF: ($x = 30, y = -6, z = 50$)

The neuronavigation procedure started with registering anatomical landmarks (nasion, inion, and ear tragus) using the neuronavigation tracker. This allowed the software to adjust the MNI average brain model, stretching and constricting it to adapt each participant's scalp. Once this was done, it was possible to view on the software the exact position of the head and coil tracker in real time. The coil was then fixed on the area, according to the coordinates, using a stable and adjustable mechanical arm designed to hold the TMS coil in place for the entire duration of the stimulation. The intensity of the stimulation was individually adjusted, using 90% of the resting motor threshold (RMT) found at the beginning of each session.

Joule heating explains the process by which the passage of an electric current through a conductor generates an amount of heat that is proportional to the square of the current, the resistance, and the

time the current flows. It is for this reason that during TMS stimulation at high intensities or for prolonged periods of time, a cooling device for the coil becomes necessary.

In this study, inhibitory rTMS at 1 Hz was used for 1500 s which required the use of such a system. The air-cooling device emitted a loud and intrusive noise, which was reduced by providing earplugs to participants before the stimulation began.

The stimulation was administered offline (i.e., while the participant was not engaging in any task), allowing us to investigate the effects of the inhibition of the targeted area on the execution of the MILO task that occurred right after.

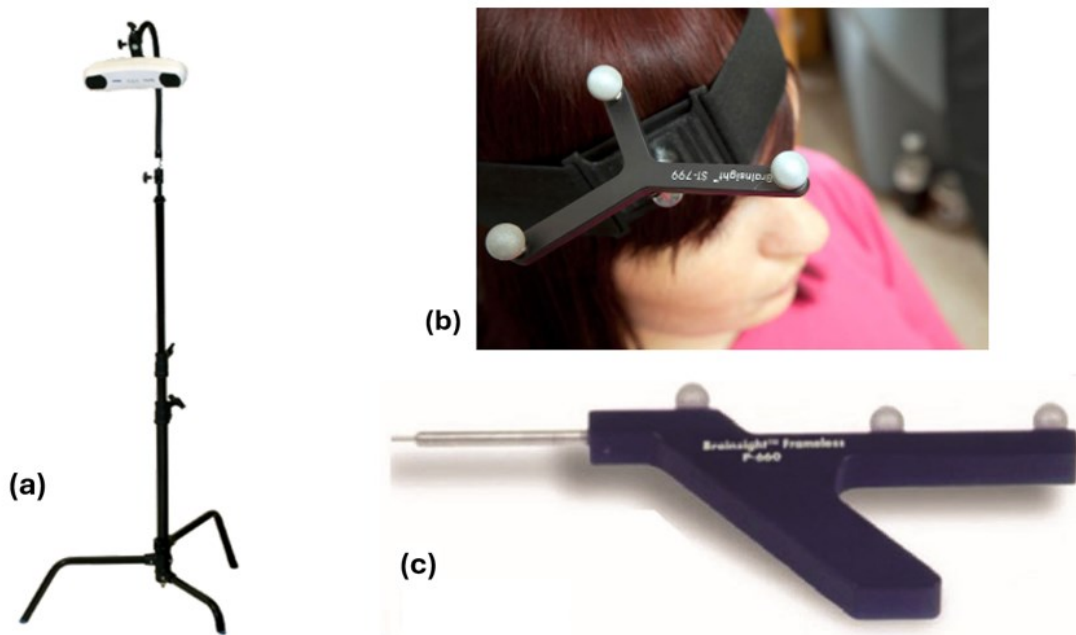


Figure 6a. Polaris infrared camera.

Figure 6b. Subject tracker and head-strap.

Figure 6c. Neuronavigation tracker.

6. Experimental Procedure and Design

The repeated-measure design consisted of three experimental sessions, with each session involving the stimulation of one of the three sites of interest (i.e., lFEF, Cz, rFEF).

The order of the sites was randomized for every participant with Cz serving as each participant's own control condition because stimulation at this site was expected to produce no significant change in the MILO task performance. Each session was scheduled at least two days apart to avoid any long-lasting interference of the TMS stimulation.

The room conditions were systematically kept constant: temperature was controlled and dim illumination was chosen to avoid reflections on the screen.

Before each session, calibration of the neuronavigational tools was performed to ensure their maximal precision.

At the beginning of each session, the RMT was determined so that stimulation was administered at the correct intensity. In absence of EMG recordings that could keep track of the MEPs, the RMT is determined through a visual inspection of the muscle twitches induced by the stimulation on the motor cortex.

We started by taking the participant's scalp measurements to locate Cz at the intersection of the lines connecting theinion to the nasion and the tragus of the left ear to the tragus of the right ear.

This site was marked with a red dot sticker.

Afterwards, to find the primary motor cortex (M1), a 3x3 grid of dot stickers was centered at 3 cm from the vertex on the hemisphere contralateral to the dominant hand.

To enhance the visualization of the MEP, the participant is instructed to rest their dominant hand on their thigh while applying slight pressure between the thumb and index finger. This position

recruits the use of the thenar eminence (i.e., a group of hand muscles responsible for movement of the thumb), making it easier to observe a muscle twitch.

The Magstim Rapid² was configured to a single pulse setting, with maximum stimulator output (MSO) of 65%. The initial intensity was adjusted starting from this level, depending on the individual's sensitivity to the stimulation by increasing or decreasing the MSO after the first pulse delivery. However, the MSO range was always kept below the safety threshold of 70%.

The coil was positioned at the center of the 3x3 grid and moved along the grid points. This was done to locate the optimal position where a single TMS pulse consistently elicited a visible and reliable muscle twitch.

Once this optimal position was identified, the participant was asked to relax the hand muscles. The TMS intensity was gradually lowered in steps of 5% MSO, and each reduction was followed by a pulse to assess muscle movement. The process continued until the intensity reached a level where muscle response was observed in approximately 50% of the stimulation trials.

The intensity at which this occurred represents the minimal level of TMS stimulation required to elicit an observable motor response and was taken as the RMT.

An intensity value corresponding to 90% of the RMT was used for the offline stimulation of the three sites of interest.

After determining the RMT, the participant was asked to move to the computer desk, distance from the screen was adjusted, and once the chin rest was set, the first session of the MILO 2022 task was initiated.

Upon completion of the behavioral task, the participant was provided with ear plugs and the neuronavigation procedure was carried out. When the target area was precisely located, the TMS

coil was fixed to the mechanical arm to minimize any movement from the target site during stimulation.

All participants were encouraged to immediately signal any discomfort, whether it was due to the prolonged sitting posture or the TMS, so that the session could be promptly paused or terminated.

Finally, a second session of the MILO 2022 task was conducted.

7. Results

The MILO 2022 web app automatically recorded the reaction times for each participant as they completed the task. For each administration, participants generated eight reaction times, labeled from RT1 through RT8. The time measurements were cumulative, meaning that each RT measured the total time elapsed from the beginning of the trial up to that specific target.

Therefore, RT1 represented the time elapsed between the start of the trial and the participant's click on the first target and RT8 was the total time taken to complete that trial.

To derive the SRTs, the primary dependent variable in the study, we calculated the time intervals between successive clicks. The seven SRTs were obtained by using the formula

$SRT_x = RT_{x+1} - RT_x$, reflecting the time taken from one click to the next.

Three independent variables were hypothesized to have a causal effect on the SRTs, namely the “*target number*,” “*Vanish-Remain condition*,” and “*time*.”

The “*target number*” is the number of the item in the sequence, which goes from 1 to 8.

The “*Vanish-Remain condition*” variable refers to *Vanish* or *Remain* trials and determines the visibility of the target items upon selection.

The “*time*” is intended as the moment of data collection, pre- or post- stimulation for each site, capturing the effects of the TMS on participants’ performance.

In the current study, each participant completed the MILO under both *Vanish* and *Remain* conditions and was assessed at both pre- and post- stimulation, for each of the three stimulation sites. In order to analyze the effect of each independent variable (i.e., factor) on the quantitative dependent variable (i.e., SRTs), three repeated measures analyses of variances (ANOVAs) were conducted – one for each stimulation site.

In addition, the data was further explored by analyzing the slopes of the linear regression that described the decrease in SRTs as a function of the target number (thus from target 2 to target 8, since SRTs for target 1 are in fact not related to previous target selections and are much larger than those for the following targets), using three repeated measures ANOVAs. The two factors considered for these analyses were the “*Vanish-Remain condition*” and “*time*.”

We expected to observe no significant difference in the negative slopes between the two conditions before stimulation, replicating the results of Thornton and Horowitz (2004). However, in the post-stimulation phase of the FEF areas, following the suppression of the inhibitory tagging, we should observe significantly less steep slopes in the *Remain* condition compared to the *Vanish* condition.

7.1 Factor 1 - Target Number

Overall, the variable “*target number*” was a significant factor in each stimulation condition: IFEF ($F_{6,66} = 34.12$, $p < .001$, $\eta^2 = .54$), Cz ($F_{6,66} = 49.99$, $p < .001$, $\eta^2 = .68$), and rFEF ($F_{6,66} = 23.95$, $p < .001$, $\eta^2 = .49$). On all the three stimulation sites, the SRTs significantly decreased with an increasing target number as expected (Fig. 7, 8, and 9).

Moreover, through the analysis of the interaction between the factors “*target number*” and “*Vanish-Remain condition*,” it was found that the inhibitory tagging was being employed. In particular, the absence of a significant interaction between these two factors for each site (IFEF - $F_{6,66} = 1.40$, $p = .228$; Cz - $F_{6,66} = 1.50$, $p = .192$; rFEF - $F_{6,66} = 1.47$, $p = .202$), suggests that the SRTs are not subjected to significant changes between the *Vanish* and *Remain* conditions, confirming the findings of Thornton and Horowitz (2004) and the intrinsic ability of the MILO task to evoke the inhibitory tagging mechanism.

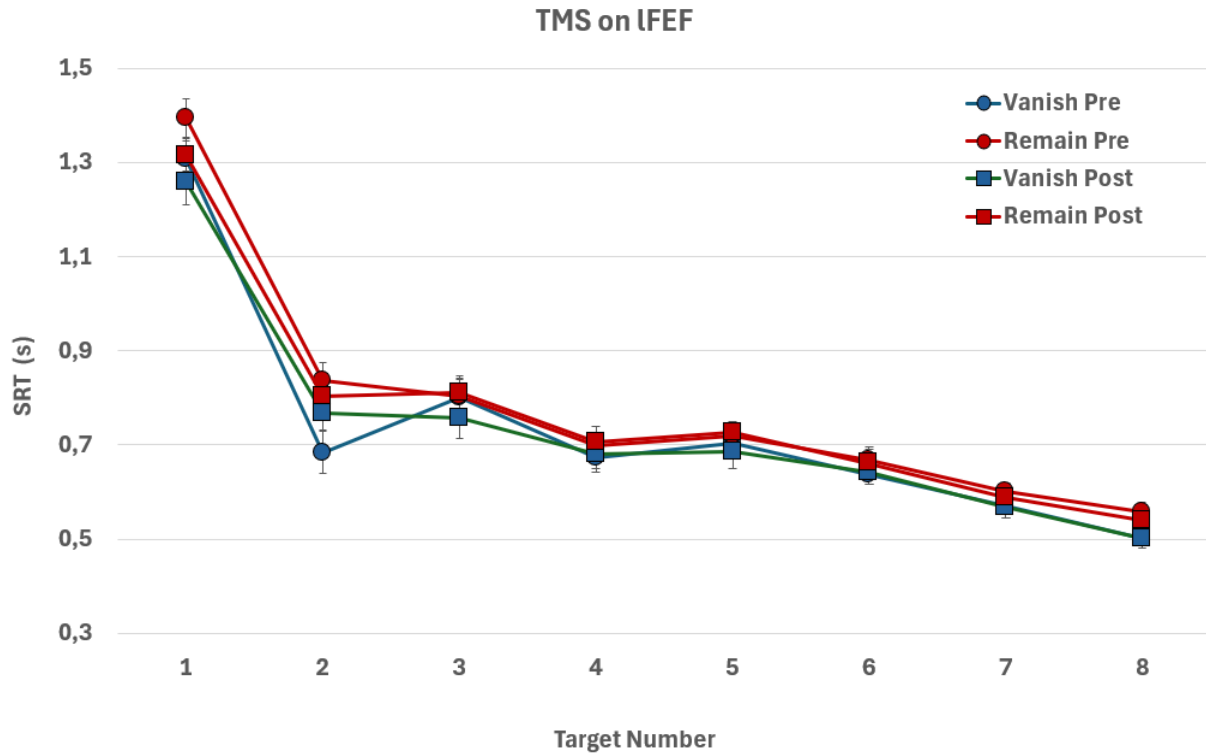


Figure 7. Line graph depicting the average SRTs for the lFEF, showing a decrease in SRTs as the target number increases. The x-axis reports the target number (1-8). The y-axis indicates the average SRT in seconds. The graph compares the mean SRTs across different conditions: vanish pre-stimulation, vanish post-stimulation, remain pre-stimulation, and remain post-stimulation.

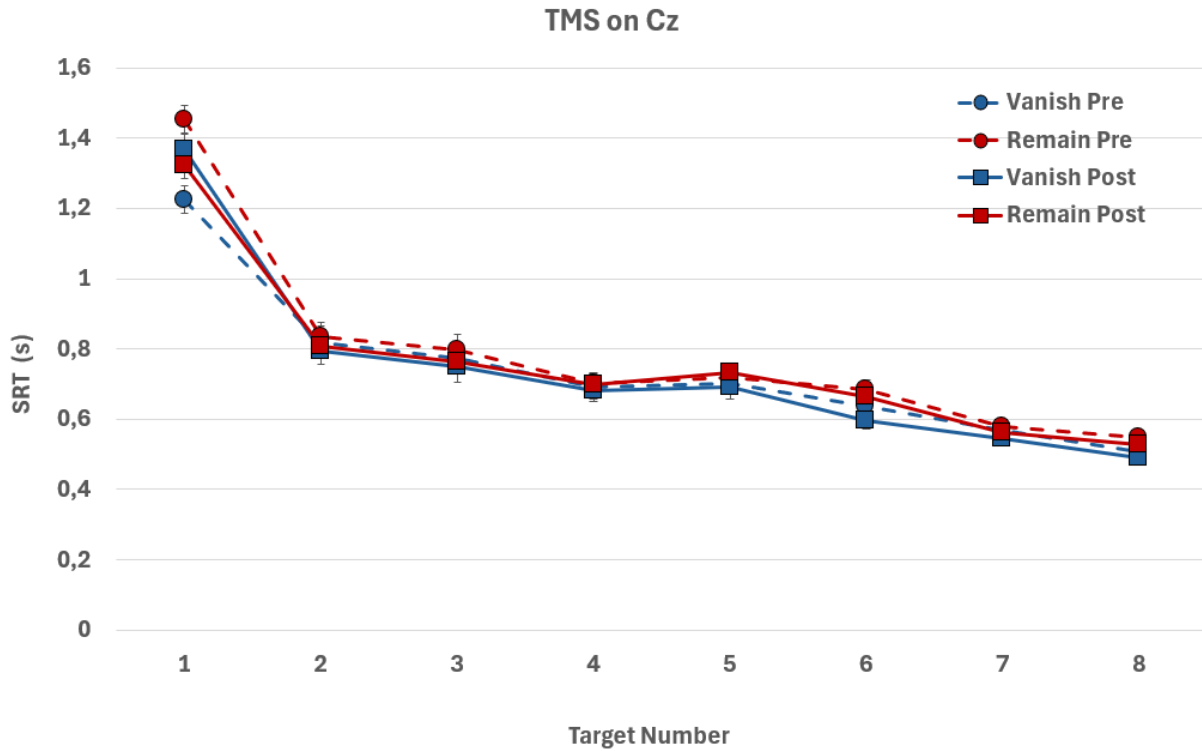


Figure 8. Line graph depicting the average SRTs for Cz, showing a decrease in SRTs as the target number increases. The x-axis reports the target number (1-8). The y-axis indicates the average SRT in seconds. The graph compares the mean SRTs across different conditions: vanish pre-stimulation, vanish post-stimulation, remain pre-stimulation, and remain post-stimulation.

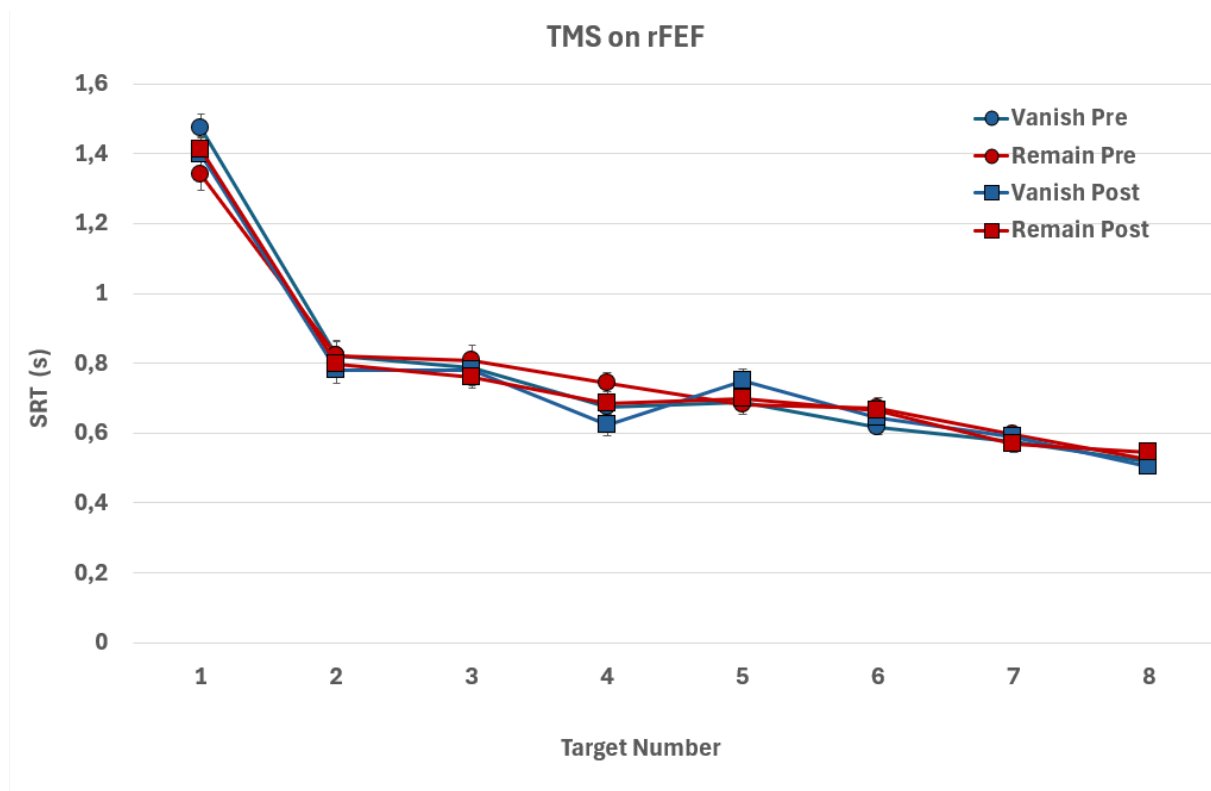


Figure 9. Line graph depicting the average SRTs for the rFEF, showing a decrease in SRTs as the target number increases. The x-axis reports the target number (1-8). The y-axis indicates the average SRT in seconds. The graph compares the mean SRTs across different conditions: vanish pre-stimulation, vanish post-stimulation, remain pre-stimulation, and remain post-stimulation.

7.2 Factor 2 - Vanish-Remain condition

The second factor analyzed was the “*Vanish-Remain condition*.” From the analysis, in both IFEF ($F_{1,11} = 28.40, p < .001, \eta^2 = .025$) and Cz ($F_{1,11} = 10.73, p = .007, \eta^2 = .012$), the *Vanish* condition was significantly faster than *Remain* condition. This effect was only marginally significant for rFEF ($F_{1,11} = 4.49, p = .058, \eta^2 = .003$).

Initially, the results may seem contradictory to the nature of the inhibitory tagging mechanism, which is thought to improve visual search efficacy by ignoring already processed targets in the *Remain* condition. However, in the *Vanish* condition, as each target is selected, the physical set size decreases, which likely reduces global visual interference from the remaining distractors. This reduction in visual interference may improve search efficiency more than the inhibitory tagging, and result in significantly faster SRTs for the *Vanish* than for the *Remain* condition.

7.3 Factor 3 - Time

The third factor analyzed was “*time*” and its effects on the SRTs. The data showed that only on Cz, the post-stimulation phase, had significantly faster SRTs than the pre-stimulation ($F_{1,11} = 5.49, p = .039, \eta^2 = .006$). It is unlikely that the inhibitory TMS stimulation on the vertex generated some type of facilitation in the visual search, hence this finding may be attributed to a practice effect. Despite the random spatial location of the targets in each trial of the MILO, participants may have become more accustomed with the experimental setting and the web app interface over time. Thus, the facilitation in visual search in the post-stimulation phase may be attributed to a growing familiarity with the task, rather than to an actual neurophysiological effect induced by the stimulation on Cz.

We had also postulated that following the stimulation of the FEF areas there would be a significant increase in SRTs due to the increased difficulty created by the suppression of the inhibitory tagging mechanism, however this did not occur (lFEF - $F_{1,11} = .013$, $p = .911$, $\eta^2 = 2.100 \times 10^{-5}$; rFEF - $F_{1,11} = .951$, $p = .350$, $\eta^2 = .001$).

7.4 Analysis of interaction effects

In the three ANOVAs conducted, none of the possible interactions obtained significance. Nonetheless, on the lFEF there is a marginally significant result for the three-way interaction “*time*” × “*Vanish-Remain condition*” × “*target number*” ($F_{6,66} = 2.05$, $p = .071$, $\eta^2 = .010$) that might suggest a role in the inhibitory tagging mechanism. However, this marginally significant result is neither supported by post-hoc tests, nor by the analyses of the slopes. Additionally, from the graph for lFEF (Fig.7) it is possible to see that differences in SRTs may tend towards significance mainly due to differences in the first few targets, and not in the later ones.

As an example:

- The average SRT for target 1 in the pre-stimulation “*Remain*” condition is 1.394 s.
- The average SRT for target 1 in the post-stimulation “*Remain*” condition is 1.316 s.

The post-stimulation “*Remain*” condition is numerically faster than the pre-stimulation “*Remain*” condition for the initial targets 1 and 2, and this trend stops for greater target numbers, where the curves describing these functions largely overlap. This suggests that the marginally significant interaction could be due to differences in the very first targets and is not indicative of any suppression of inhibitory tagging.

7.5 Analysis of the slopes

Repeated measures ANOVAs were conducted for each stimulation site on the slopes of the SRT \times target number functions using as factors “*Vanish-Remain condition*” and “*time*.” Neither of these two factors had a significant effect ($p > .05$) on the differences observed among the slopes (Fig. 10, 11 and 12). However, data shows a trend towards significance for the factor “*time*” on the rFEF ($F_{1,11} = 3.72$, $p = .08$, $\eta^2 = .095$) that occurred regardless of the “*Vanish-Remain condition*”. In particular, for both *Vanish* and *Remain* conditions the slopes tended to become less steep. This finding may be due to variations in response times to the initial items (average SRT equal to 821 ms at target 2 prior TMS vs 789 ms post TMS) rather than improvements in the inhibition of responses to the final items (average SRT equal to 521 ms at target 8 prior TMS vs 523 ms post TMS). Once again, it seems that there was no causal effect induced by the stimulation on the inhibitory tagging mechanism.



Figure 10. Boxplot showing the distribution of slopes in Vanish and Remain conditions, both pre- and post- stimulation on the IFEF. The y-axis reports the average slope in s/subsequent item.



Figure 11. Boxplot showing the distribution of slopes in Vanish and Remain conditions, both pre- and post- stimulation on Cz. The y-axis reports the average slope in s/subsequent item.

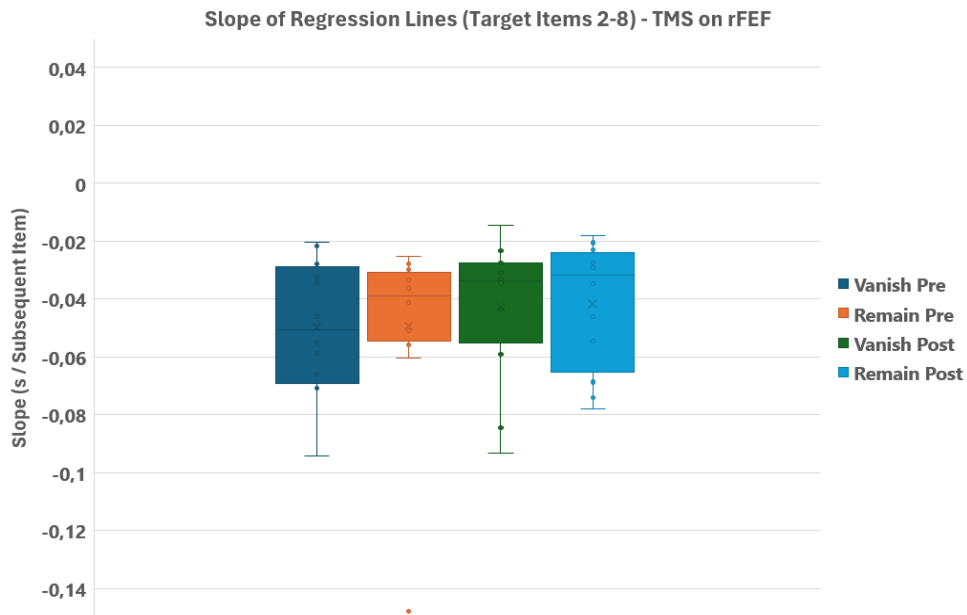


Figure 12. Boxplot showing the distribution of slopes in Vanish and Remain conditions, both pre- and post- stimulation on the rFEF. The y-axis reports the average slope in s/subsequent item.

8. Discussion and Conclusions

The findings reported did not support a causal relationship linking the TMS stimulation of the FEF areas to a worsening of the performance on the MILO, especially in the last targets of the sequence in the *Remain* condition.

However, the significance of the “*target number*” factor along with the non-significant interaction between this and “*Vanish-Remain condition*” confirmed the results of Thornton and Horowitz (2004).

The gradual decrease in SRTs occurred independently of the two conditions, *Vanish* and *Remain*, exactly as their study reported.

In the post-stimulation phase, we found no evidence supporting the suppression of the inhibitory tagging mechanism. Nonetheless, the analyses of the slopes revealed a trend towards significance on the rFEF in the expected direction, with the post-stimulation phase having more positive slopes, thus a poorer search efficacy. This would be attributed to disruption of the inhibitory tagging, if the factor “*Vanish-Remain condition*” were to be significant and if the change in slope was mainly due to longer SRTs in the last targets of the sequence, neither of which occurred.

Therefore, we cannot draw definitive conclusions about the neural correlates of this attentional mechanism.

Several factors may have contributed to these results. First, despite relying on a recent meta-analysis, the precise localization of the FEF areas in humans remains controversial as most studies adopt functional localization methods, without accurately knowing their contribution to cognitive aspects of visual attention or which subregions are responsible for which functions. Moreover, optimal neuronavigation requires participants’ MRI scans to generate a more precise brain reconstruction on the software. The adaptation of the MNI brain template to the participants’ scalp

measurements may have overlooked the variability between individual brains, which seems to be fundamental in context.

Finally, the inhibitory tagging mechanism may not be an exclusive function of the FEF areas, but rather a feature of the frontoparietal attentional network. Therefore, a more detailed analysis of this network could offer greater insights into their role in visual attention.

9. References

- Barrett, A. M. (2021). Spatial neglect and anosognosia after right brain stroke. *CONTINUUM Lifelong Learning in Neurology*, 27(6), 1624–1645.
<https://doi.org/10.1212/con.0000000000001076>
- Bedini, M., Olivetti, E., Avesani, P., & Baldauf, D. (2023). Accurate localization and coactivation profiles of the frontal eye field and inferior frontal junction: an ALE and MACM fMRI meta-analysis. *Brain Structure and Function*, 228(3–4), 997–1017.
<https://doi.org/10.1007/s00429-023-02641-y>
- Bisley, J. W. (2010). The neural basis of visual attention. *Journal of Physiology*, 589(1), 49–57. <https://doi.org/10.1113/jphysiol.2010.192666>
- Broadbent, D. E. (1958). Perception and communication. In *Pergamon Press eBooks*.
<https://doi.org/10.1037/10037-000>
- Corbetta, M., Kincade, J. M., Ollinger, J. M., McAvoy, M. P., & Shulman, G. L. (2000). Voluntary orienting is dissociated from target detection in human posterior parietal cortex. *Nature Neuroscience*, 3(3), 292–297. <https://doi.org/10.1038/73009>
- Corbetta, M., & Shulman, G. L. (2002). Control of goal-directed and stimulus-driven attention in the brain. *Nature Reviews. Neuroscience*, 3(3), 201–215.
<https://doi.org/10.1038/nrn755>
- Klein, R. (1988). Inhibitory tagging system facilitates visual search. *Nature*, 334(6181), 430–431. <https://doi.org/10.1038/334430a0>
- Klein, R. M. (2000). Inhibition of return. *Trends in Cognitive Sciences*, 4(4), 138–147.
[https://doi.org/10.1016/s1364-6613\(00\)01452-2](https://doi.org/10.1016/s1364-6613(00)01452-2)

- Koponen, L. M., & Peterchev, A. V. (2020). Transcranial magnetic stimulation: principles and applications. In *Springer eBooks* (pp. 245–270). https://doi.org/10.1007/978-3-030-43395-6_7
- Lefaucheur, J. (2019). Transcranial magnetic stimulation. In *Handbook of clinical neurology* (pp. 559–580). <https://doi.org/10.1016/b978-0-444-64032-1.00037-0>
- Mather, G. (2016). *Foundations of sensation and perception*. Psychology Press.
- Mirpour, K., Bolandnazar, Z., & Bisley, J. W. (2019). Neurons in FEF keep track of items that have been previously fixated in free viewing visual search. *Journal of Neuroscience*, 39(11), 2114–2124. <https://doi.org/10.1523/jneurosci.1767-18.2018>
- Ro, T., Farnè, A., & Chang, E. (2003). Inhibition of return and the human frontal eye fields. *Experimental Brain Research*, 150(3), 290–296. <https://doi.org/10.1007/s00221-003-1470-0>
- Rossi, S., Antal, A., Bestmann, S., Bikson, M., Brewer, C., Brockmüller, J., Carpenter, L. L., Cincotta, M., Chen, R., Daskalakis, J. D., Di Lazzaro, V., Fox, M. D., George, M. S., Gilbert, D., Kimiskidis, V. K., Koch, G., Ilmoniemi, R. J., Lefaucheur, J. P., Leocani, L., . . . Hallett, M. (2021). Safety and recommendations for TMS use in healthy subjects and patient populations, with updates on training, ethical and regulatory issues: Expert Guidelines. *Clinical Neurophysiology*, 132(1), 269–306. <https://doi.org/10.1016/j.clinph.2020.10.003>

- Rossini, P. M., Burke, D., Chen, R., Cohen, L. G., Daskalakis, Z., Di Iorio, R., Di Lazzaro, V., Ferreri, F., Fitzgerald, P. B., George, M. S., Hallett, M., Lefaucheur, J. P., Langguth, B., Matsumoto, H., Miniussi, C., Nitsche, M. A., Pascual-Leone, A., Paulus, W., Rossi, S., . . . Ziemann, U. (2015). Non-invasive electrical and magnetic stimulation of the brain, spinal cord, roots and peripheral nerves: Basic principles and procedures for routine clinical and research application. An updated report from an I.F.C.N. Committee. *Clinical Neurophysiology*, 126(6), 1071–1107. <https://doi.org/10.1016/j.clinph.2015.02.001>
- Thornton, I. M., & Horowitz, T. S. (2004). The multi-item localization (MILO) task: Measuring the spatiotemporal context of vision for action. *Perception & Psychophysics*, 66(1), 38–50. <https://doi.org/10.3758/bf03194859>
- Vernet, M., Quentin, R., Chanes, L., Mitsumasu, A., & Valero-Cabré, A. (2014). Frontal eye field, where art thou? Anatomy, function, and non-invasive manipulation of frontal regions involved in eye movements and associated cognitive operations. *Frontiers in Integrative Neuroscience*, 8. <https://doi.org/10.3389/fnint.2014.00066>
- Vossel, S., Geng, J. J., & Fink, G. R. (2013). Dorsal and ventral attention systems. *Neuroscientist*, 20(2), 150–159. <https://doi.org/10.1177/1073858413494269>
- Wardak, C., Ibos, G., Duhamel, J., & Olivier, E. (2006). Contribution of the monkey frontal eye field to covert visual attention. *Journal of Neuroscience*, 26(16), 4228–4235. <https://doi.org/10.1523/jneurosci.3336-05.2006>